Identification of tumor-initiating cells in a highly aggressive brain tumor using promoter activity of nucleostemin

Akira Tamase[a,b,1], Teruyuki Muraguchi[a,1], Kazuhito Naka[a,1], Shingo Tanaka[a,b], Masashi Kinoshita[b], Takayuki Hoshii[a], Masako Ohmura[a], Haruhiko Shugo[a], Takako Ooshio[a,c], Mitsutoshi Nakada[b], Kazunobu Sawamoto[d], Masafumi Onodera[e], Kunio Matsumoto[f], Masanobu Oshima[g], Masahide Asano[h], Hideyuki Saya[i], Hideyuki Okano[j], Toshio Suda[k], Jun-ichiro Hamada[b], and Atsushi Hirao[a,c,2]

[a]Division of Molecular Genetics, Center for Cancer and Stem Cell Research, Cancer Research Institute, Kanazawa University, Kanazawa, Ishikawa 920-0934, Japan; [b]Department of Neurosurgery, Graduate School of Medical Science, Kanazawa University, Kanazawa, Ishikawa 920-8641, Japan; [c]Core Research for Evolutional Science and Technology, Japan Science and Technology Agency, Kawaguchi, Saitama 332-0012, Japan; [d]Department of Developmental and Regenerative Biology, Institute of Molecular Medicine, Nagoya City University Graduate School of Medical Sciences, Mizuho-ku, Nagoya 467-8601, Japan; [e]Laboratory of Genetic Diagnosis and Gene Therapy, Department of Genetics, National Research Institute for Child Health and Development, Setagaya-ku, Tokyo 157-8535, Japan; [f]Division of Tumor Dynamics and Regulation and [g]Division of Genetics, Cancer Research Institute and [h]Division of Transgenic Animal Science, Advanced Science Research Center, Kanazawa University, Kanazawa, Ishikawa, 920-8640, Japan; and [i]Division of Gene Regulation, Institute for Advanced Medical Research and Departments of [j]Physiology and [k]Cell Differentiation, The Sakaguchi Laboratory of Developmental Biology, Keio University School of Medicine, Shinjuku-ku, Tokyo 160-8582, Japan

Edited by Tak Wah Mak, Princess Margaret Hospital, Toronto, Canada, and approved August 12, 2009 (received for review May 7, 2009)

Controversy remains over whether the cancer stem cell (CSC) theory applies to all tumors. To determine whether cells within a highly aggressive solid tumor are stochastically or hierarchically organized, we combined a reporter system where the nucleostemin (NS) promoter drives GFP expression (termed NS-GFP) with a mouse brain tumor model induced by retroviral Ras expression on a p16^{Ink4a}/p19^{Arf}-deficient background. The NS-GFP system allowed us to monitor the differentiation process of normal neural stem/precursor cells by analyzing GFP fluorescence intensity. In tumor-bearing mice, despite the very high frequency of tumorigenic cells, we successfully identified the NS-GFP$^+$ cells as tumor-initiating cells (T-ICs). The clonal studies conclusively established that phenotypical heterogeneity can exist among the cells comprising a genetically homogeneous tumor, suggesting that this aggressive brain tumor follows the CSC model. Detailed analyses of the NS-GFP$^+$ brain tumor cells revealed that T-ICs showed activation of the receptor tyrosine kinase c-Met, which functions in tumor invasiveness. Thus, the NS-GFP system provides a powerful tool to elucidate stem cell biology in normal and malignant tissues.

cancer stem cell | invasion

Recent improvements in cell purification and transplantation techniques have contributed to the identification of cell populations known as tumor-initiating cells (T-ICs). These findings led to the idea that tumors are organized as hierarchies of cells sustained by such T-ICs, conceptually termed cancer stem cells (CSCs) (1, 2). Supporting this idea, in vivo models in which leukemia is initiated from primary human hematopoietic cells revealed that disease is sustained by leukemia-initiating cells (L-ICs) and that the L-ICs retain both myeloid and lymphoid lineage potential (3). Although many human malignancies appear to contain only rare tumorigenic cells or T-ICs when transplanted into NOD/SCID mice (4–6), the question of whether NOD/SCID assays underestimate the frequency of human tumorigenic cells due to differences between human and murine tissues has been raised. Recently, Quintana et al. (7) reported that ≈25% of unselected human melanoma cells from patients formed tumors when transplanted into highly immunocompromised NOD/SCID interleukin-2 receptor gamma chain null (Il2r$\gamma^{-/-}$) mice, in contrast to the very few T-ICs identified when the melanoma cells were transplanted into NOD/SCID mice (6). These results suggest that cells comprising human melanomas may constitute a homogeneous population and that any melanoma cells can form a tumor, i.e., that a hierarchical organization of tumor cells does not exist. Alternatively, it is also possible that, although T-IC frequency is very high in the melanoma, a true hierarchy exists in the aggressive tumor, because 75% of the tumor cells lack T-IC activity. It therefore remains controversial whether the cancer stem cell theory applies to all tumors (2). In our study, we have attempted to resolve this issue by examining the frequency of tumorigenic cells present in a highly aggressive murine solid tumor orthotopically transplanted into recipient mice. Our approach thus avoids the underestimation of tumorigenic cell frequency that might arise due to environmental differences between human and mouse tissues.

To investigate whether murine brain tumors exhibit cellular heterogeneity, we took advantage of our unique NS-GFP stem cell-marking system, in which the green fluorescent protein (GFP) is expressed under the control of promoter of the nucleostemin (NS) gene (8). The NS, a nucleolar GTPase, is found at high levels in various tissue stem cells and cancer cells (9). Because NS expression decreases rapidly in stem cells when these cells differentiate before cell cycle exit, it has been suggested that the NS protein is a marker for proliferating cells in an early multipotential state (9, 10). In the regenerating newt lens, the NS protein rapidly accumulates in the nucleoli of dedifferentiating pigmented epithelial cells (11), suggesting that NS expression correlates with undifferentiated status of cells. Previously, we generated NS-GFP transgenic (NS-GFP-Tg) mice and used these mice to identify a fraction of neonatal germ cells as spermatogonial stem cells (8). In the present study, we have combined our NS-GFP-Tg system with a murine brain tumor model to investigate whether aggressive solid tumors contain a distinct population of T-ICs.

Results

High Frequency of Tumorigenic Cells in an Aggressive Murine Brain Tumor. T-ICs have been identified in human high-grade gliomas (glioblastoma multiforme), which are very aggressive, invasive, and

Author contributions: A.H. designed research; A.T., T.M., K.N., S.T., M.K., T.H., M. Ohmura, H. Shugo, and T.O. performed research; M. Onodera, K.M., and M.A. contributed new reagents/analytic tools; M.N., K.S., M. Oshima, H. Saya, H.O., T.S., J.-i.H., and A.H. analyzed data; and A.T. and A.H. wrote the paper.

The authors declare no conflict of interest.

This article is a PNAS Direct Submission.

[1]A.T., T.M., and K.N. contributed equally to this work.

[2]To whom correspondence should be addressed. E-mail: ahirao@kenroku.kanazawa-u.ac.jp.

This article contains supporting information online at www.pnas.org/cgi/content/full/0905016106/DCSupplemental.

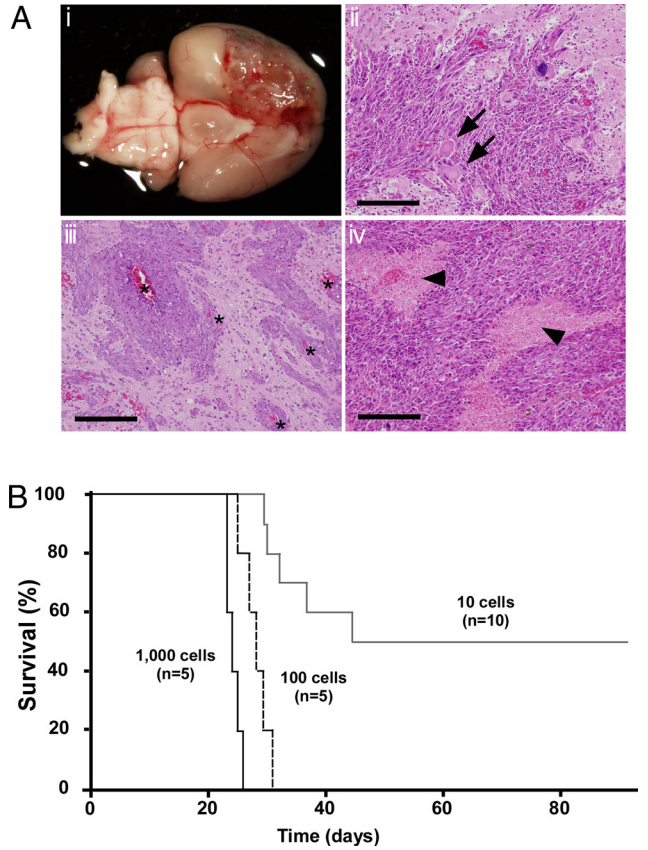

Fig. 1. High frequency of tumorigenic cells in a murine brain tumor. (*A*) Development of brain tumors. (*i*) Gross appearance of a recipient brain. A massive lesion can be seen in the cerebrum. (*ii–iv*) H&E staining of representative sections of brain tumors. Regions of increased cell density, nuclear pleomorphism, and prominent mitotic figures can be seen. Arrows, giant cells; arrowheads, areas of necrosis with pseudopalisading; asterisks, invading tumor cells adjacent to blood vessels. (Scale bars: 200 μm.) (*B*) Survival of recipient mice after transplantation of 1,000, 100, or 10 huKO$^+$ tumor cells, as indicated.

destructive brain tumors (12). Invasive tumor cells escape surgical removal and geographically dodge lethal radiation exposure and chemotherapy. A mouse brain tumor model of human glioblastoma multiforme can be generated by triggering Ras signaling downstream of the epidermal growth factor (EGF) receptor in brain cells of mice deficient for the tumor suppressors p16^{Ink4a}/p19^{Arf} (13–15). We modified the reported protocol (15) and constructed a vector containing a constitutively active mutant K-ras gene (K-ras^{G12V}) plus the humanized Kusabira-Orange (huKO) gene as a marker. We used retroviral infection to introduce this vector into cultured neurospheres composed of neural stem cells and precursor cells (NSC/NPCs) derived from the subventricular zone (SVZ) of brains of neonatal p16$^{Ink4a-/-}$/p19$^{Arf-/-}$ mice. The infected neurospheres were then injected into the basal ganglia of wild type (WT) recipient mice (Fig. S1). Brain tumors developed as early as 20 days after transplantation, and most recipients died within 40 days of injection. Consistent with previous reports (13–16), histological analyses of these tumors demonstrated that these tumors showed several features characteristic of human gliomas (17), including microvascular proliferation, the presence of giant cells, and/or areas of tumor necrosis bordered by dense palisades of viable tumor cells (necrosis with pseudopalisading) (Fig. 1*A*).

To analyze the frequency of T-ICs within tumors, the malignancies were recovered from recipients and dissociated by collagenase treatment. To eliminate any contaminating normal brain cells, flow cytometry was used to collect huKO$^+$ cells (i.e., cells overexpressing K-ras^{G12V}). Transplantation of 100 or 1,000 freshly isolated tumor cells into the brains of WT mice (8 weeks old) resulted in brain tumor formation in 100% of recipients (Fig. 1*B*). Even when only 10 tumor cells were injected, 50% of recipients developed brain tumors, suggesting that the frequency of tumorigenic cells in the original tumor was very high.

Correlation of In Vivo Differentiation Status of NSC/NPC and GFP Fluorescence Intensity in NS-GFP-Tg Brain. Tsai and McKay have reported that NS is highly expressed in undifferentiated NSC/NPCs but not in differentiating neurons (9). To determine whether the NS-GFP system marked NSC/NPCs, we evaluated GFP expression in embryonic brains of our NS-GFP-Tg mice. In embryonic brain at E14.5, radial glial cells in the ventricular zone are NSC/NPCs. At this stage, the cortical plate is formed by active neurogenesis derived from NSC/NPCs (18). In the NS-GFP-Tg brain at E14.5, higher GFP expression was observed in ventricular zone cells expressing nestin (19) or musashi-1 (20), a protein enriched in NSC/NPCs, whereas TuJ1$^+$ neurons showed a lower level of GFP (Fig. 2*A* and Fig. S2). In neonatal brain (P3), GFP was highly expressed in SVZ, which are actively cycling, and down-regulated in the striatum (Fig. S3). These analyses suggested that NSC/NPCs are included within the subpopulation of normal brain cells that expresses high levels of GFP.

To investigate the relationship between GFP fluorescence intensity and cellular properties, we used flow cytometry to divide the total cell population recovered from dissociated E14.5 NS-GFP-Tg brains into four fractions according to GFP fluorescence intensity: GFP$^{-/+}$, GFP^{++}, GFP^{+++} and GFP^{++++} (Fig. 2*B*). Immunostaining of the sorted cells with anti-nestin or anti-TuJ1 revealed that most GFP^{++++} cells expressed nestin but not TuJ1 (Fig. 2*C*), indicating that they were undifferentiated. In contrast, GFP$^{-/+}$ cells expressed TuJ1 but not nestin. Thus, our NS-GFP-Tg system allows us to monitor stem cell differentiation during neurogenesis. When we examined the capacity of our four GFP-expressing subpopulations to form neurospheres, we found that neurosphere-initiating cells were most efficiently generated by cells with higher GFP expression, whether these cells were derived from embryonic (E14.5) or neonatal (P3) NS-GFP-Tg brains (Fig. 2 *D–F*). In particular, half of the total neurosphere-initiating cells in neonatal brain were enriched in the rare (10%) GFP^{++++} cell population. Our findings support previous reports showing that neurosphere-initiating cells are enriched in sorted GFP-strong positive cells isolated from the brains of *nestin*-EGFP mice (21). We conclude that brain cells in our NS-GFP system that express very high levels of GFP exhibit a substantial capacity for both proliferation and NSC/NPC differentiation.

Identification of Brain T-ICs. Our success in monitoring normal NSC/NPC differentiation in NS-GFP-Tg mice prompted us to use this system to analyze cellular heterogeneity in our brain tumor model. We crossed our NS-GFP-Tg mice to p16$^{Ink4a-/-}$/p19$^{Arf-/-}$ mice and induced the generation of brain tumors as described above. Flow cytometric analyses of these huKO$^+$ tumors derived from NS-GFP-Tg mice revealed that they contained both GFP^{high} and GFP^{low} populations. The ratio of GFP^{high} to GFP^{low} cells was highly variable among individual tumors (Fig. 3*A*). Immunocytochemical analysis of freshly isolated tumor cells confirmed that endogenous NS was highly expressed in GFP^{high} cells but not in GFP^{low} cells (Fig. S4). CD133 (prominin 1) or nestin has been reported to be a marker of T-ICs in human glioma. The expression pattern of prominin 1 mRNA varied among tumors (Fig. S5); however, we found that GFP^{high} cells primarily expressed nestin, whereas the GFP^{low} population showed nestin down-regulation (Fig. 3*B*). These data suggested that the GFP^{high} tumor cells might be immature cells with the potential to differentiate into GFP^{low} tumor cells in vivo.

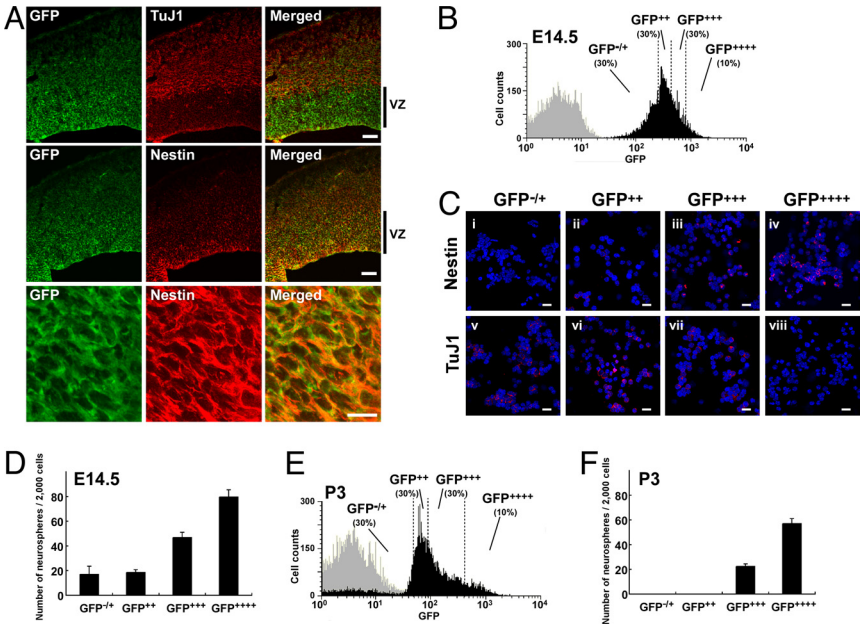

Fig. 2. Correlation of in vivo differentiation status of NSC/NPC and GFP fluorescence intensity in the NS-GFP-Tg brain. (*A*) High GFP expression correlates with high nestin expression in cells of NS-GFP-Tg embryonic forebrains. Coronal sections of forebrains of E14.5 NS-GFP-Tg mice were subjected to immunohistochemical analysis using anti-GFP (green) plus anti-type III β-tubulin (TuJ1; red, *Top*), or anti-GFP plus anti-nestin (red, *Middle* and *Bottom*). Images of the ventricular zone (VZ) cells in the *Middle* are shown at higher magnification in *Bottom*. (Scale bars: *Top* and *Middle*, 100 μm; *Bottom*, 10 μm). (*B*) Fractionation of GFP-expressing cells from E14.5 NS-GFP-Tg brain. Total brain cells from E14.5 NS-GFP-Tg mice were dissociated and fractionated by flow cytometry into 4 subpopulations, $GFP^{-/+}$, GFP^{++}, GFP^{+++} and GFP^{++++}, based on GFP fluorescence intensity as indicated. Gray peak, WT C57BL/6 mice; black peak, NS-GFP-Tg mice. (*C*) Correlation of high GFP expression with immature cell properties. The fractionated brain cell subpopulations from *B* were fixed and analyzed by immunocytochemistry to detect expression of nestin (red, *i–iv*) or TuJ1 (red, *v–viii*) as indicated. Blue, nuclear marker TOTO-3. (Scale bars, 20 μm.) (*D*) Correlation of GFP expression with neurosphere-forming capacity in E14.5 NS-GFP-Tg brain tissues. Fractionated brain cell subpopulations from *B* were cultured under conditions allowing neurosphere formation. Data shown are the mean number ± SD. of neurospheres generated per 2,000 cells (n = 3 per group). (*E*) Fractionation of P3 GFP-expressing brain cells. Total brain cells from P3 NS-GFP-Tg mice were dissociated and fractionated by flow cytometry into 4 subpopulations, $GFP^{-/+}$, GFP^{++}, GFP^{+++} and GFP^{++++}, based on GFP fluorescence intensity as indicated. Gray peak, WT C57BL/6 mice; black peak, NS-GFP-Tg mice. (*F*) Correlation of GFP expression with neurosphere-forming capacity in P3 NS-GFP-Tg brain tissues. The fractionated brain cell subpopulations in *E* were cultured to allow neurosphere formation as for *D*. Data shown are the mean number ± SD. of neurospheres generated per 2,000 cells (n = 3 per group).

To investigate the properties of the GFP^{high} and GFP^{low} tumor cells, we first evaluated their capacity to form spheres in culture. Many spheres were generated in cultures of GFP^{high} cells, whereas GFP^{low} cells produced only a few spheres (Fig. 3*C*). To investigate the behavior of the GFP^{high} and GFP^{low} tumor cells in vivo, the cells were orthotopically transplanted into WT mice to generate new brain tumors. All mice receiving 10,000 GFP^{high} cells developed brain tumors (Fig. 3*D*). However, the frequency of tumorigenicity was decreased and tumor onset was delayed in mice that received 10,000 GFP^{low} tumor cells. Because it was possible that the GFP^{low} cell population had been contaminated by a very small number of GFP^{high} cells, the transplant cell number was reduced to eliminate the possibility of contamination. No tumor arose in recipients even when 1,000 GFP^{low} cells were transplanted, but injection of 1,000 or 100 GFP^{high} cells was sufficient to generate brain tumors in 100% of recipients. When only 10 tumor cells were injected, 60% of recipients developed brain tumors. Thus, our NS-GFP system significantly distinguishes tumorigenic from nontumorigenic cells.

We next explored the cellular heterogeneity of tumors developing in WT recipient brains. Histological analysis showed that malignancies developing in WT mice that had received 10 GFP^{high} tumor cells tended to show less morphological variability than the original brain tumors (Fig. 3*E*), suggesting that the latter may have arisen from multiple clones with different retrovirus integration sites. Nonetheless, the pattern of GFP expression in cells of the transplanted tumors was similar to that in the original tumors, in that secondary tumors also had both GFP^{high} and GFP^{low} populations (Fig. 3*E*). Because the brain tumors generated by injection of 10 GFP^{high} tumor cells were not necessarily of single-cell origin, we performed limiting dilution experiments on the original tumors to isolate single cell-derived tumors. All neurospheres derived from such single tumor cells exhibited bright GFP fluorescence (Fig. 3*F*). When such GFP^{bright} neurospheres were injected into WT recipient mice, the resulting brain tumors also contained GFP^{high} and GFP^{low} tumor cells and therefore recapitulated the original GFP expression pattern (Fig. 3*G*). These clonal studies conclusively establish that bona fide functional heterogeneity can exist among cells comprising a genetically homogeneous tumor, and T-ICs can be identified in highly aggressive tumors.

Invasiveness of T-ICs. To better understand T-IC behavior, we used our NS-GFP-Tg brain tumor model to track the localization of GFP^{high} tumor cells in vivo. Immunohistochemical analyses of sections of either the single-cell-derived tumors or the original tumors showed the tumor cells expressing GFP (GFP^{+} cells) were localized predominantly in the areas of the tumor facing normal tissues (Fig. 4 *A*, *B*, and *D*), whereas tumor cells located in center of the malignancy did not express GFP (Fig. 4*C* and Fig. S6). Scattered GFP^{+} tumor cells also invaded the normal brain tissue adjacent to the tumor (Fig. 4 *B* and *D*). A typical feature of human gliomas is the spreading of tumor cells along the basement membranes of blood vessels. As shown in Fig. 4 *E* and *F*, blood vessels adjacent to the tumor were surrounded by GFP^{+} cells, suggesting that these T-ICs drive the invasion of the malignancy into normal brain tissues.

We next compared GFP^{high} and GFP^{low} cells from brain tumors for expression of genes responsible for tumor cell migration and invasion. We found that c-Met, a receptor tyrosine kinase that binds hepatocyte growth factor (HGF), was expressed at much higher levels in the GFP^{high} cells of a given tumor than in the tumor's GFP^{low} cells (Fig. 5*A*). HGF, originally identified as a mitogen for hepatocytes, potently enhances dissociation of cell–cell adhesiveness, cell motility, and extracellular matrix breakdown, thereby promoting tumor cell invasion and metastasis (22, 23). Several studies suggest that inhibition of the HGF/c-Met pathway is of therapeutic benefit in cases of human glioma (24–26). When we carried out immunohistochemical analyses of our brain tumors, we found that c-Met was phosphorylated in GFP^{+} tumor cells at the invasion front of the malignancy (Fig. 5*B*), indicating that the T-ICs showed activation of c-Met signal. To analyze whether these T-ICs indeed have potential for migration in response to c-Met/HGF signaling, we inoculated tumor cells into a collagen gel containing HGF. Although HGF did not affect number of sphere formation, it dramatically induced the migration and elongation of GFP^{+}

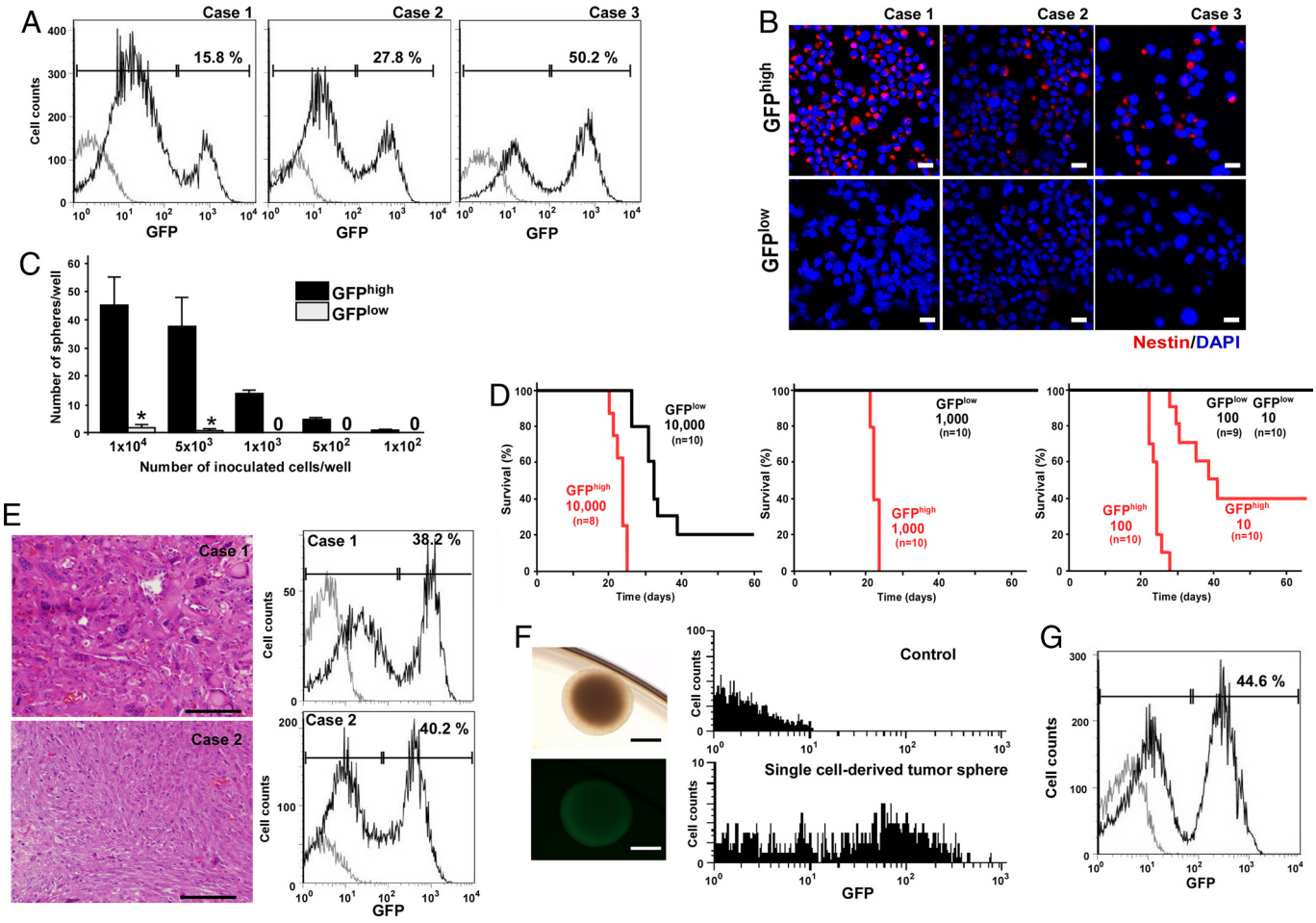

Fig. 3. Identification of T-ICs. (*A*) Detection of GFP^{high} and GFP^{low} subpopulations among brain tumor cells derived from NS-GFP-Tg mice. Tumors were dissociated with collagenase and GFP expression was analyzed in huKO^{+} tumor cells by flow cytometry. Tumors contained variable percentages of GFP^{high} and GFP^{low} cells. Three representative samples showing the GFP expression pattern in huKO^{+} tumor cells are shown. (*B*) GFP^{high} tumor cells exhibit immature cell properties. Cytospin smears of sorted GFP^{high} and GFP^{low} cells in *A* were fixed and immunostained to detect nestin (red). Blue, nuclear marker DAPI. Three representative samples of 5 independent experiments are shown. (Scale bars: 20 μm.) (*C*) GFP^{high} tumor cells can generate spheres. GFP^{high} and GFP^{low} cells from brain tumors in *A* were cultured for 14 days under sphere formation conditions. Data shown are the mean number ± SD. of spheres per indicated number of inoculated cells ($n = 4$ per group; *, $P < 0.01$). (*D*) Transplantation of GFP^{high} brain tumor cells curtails survival. The percentage survival of WT recipient mice injected with 10,000, 1,000, 100, or 10 GFP^{high} or GFP^{low} brain tumor cells is shown as indicated. (*E*) Maintenance of the GFP expression pattern between original and transplanted brain tumors. Analysis of histology (by H&E staining, *Left*) and GFP expression (by flow cytometry, *Right*) of brain tumors isolated from two WT recipient mice transplanted with 10 GFP^{high} brain tumor cells (as from *D*, *Right*). (Scale bars: 200 μm.) (*F*) A neurosphere derived from a single tumor cell by limiting dilution. (*Left Upper*) Bright field. (*Left Lower*) GFP fluorescence. (Scale bars: 200 μm.) *Right*, GFP fluorescence as determined by flow cytometry. (*Upper*) Neurospheres from control mice (P3). (*Lower*) Single cell-derived spheres from NS-GFP tumor. Representative data are shown. (*G*) Maintenance of GFP expression pattern between original tumors and tumors arising from transplantation of single-cell-derived neurospheres. Neurospheres derived in culture from single cells of an original tumor were transplanted into WT recipient mice. Tumors arising in these recipients were dissociated and the expression of their component cells analyzed. Data representative of 4 independent experiments are shown.

T-ICs placed in a collagen gel (Fig. 5*C*). These T-ICs therefore have the potential to respond to HGF and migrate through a matrix with collagenase activity. These data suggest that the T-ICs identified by our NS-GFP-Tg system lead the invasion of the malignancy into normal brain tissue.

Discussion

In this study, we used a murine brain tumor model to establish that even in aggressive brain tumors that contain a high frequency of T-ICs, T-ICs represent a distinct cell type capable of generating non-T-ICs, which comprise the bulk of the tumor tissue. The use of a syngenic and orthotopic system overcomes limitations of xenotransplant systems, which typically show relatively low frequencies of T-ICs in human brain tumors (5). The concern that environmental differences existing between human and mouse tissues might lead to an underestimation of tumorigenic cell frequency may be supported by our data. It could be argued that our tumor model is more aggressive than a spontaneous tumor because we generate malignancies by oncogene overexpression. However, although the tumors were generated experimentally, histological analyses demonstrate that these tumors exhibit apparent heterogeneity, similar to human gliomas. Our results clearly demonstrate that, if the appropriate marker is available, T-ICs can be identified in an aggressive solid tumor regardless of their frequency.

Optimization of xenotransplantation assays by using highly immunocompromised NOD/SCID/Il2r$\gamma^{-/-}$ mice dramatically improved the transplantation efficiency of human melanoma cells, compared with traditional NOD/SCID mice (7), suggesting that the human melanoma randomly form tumor in the mice or genetic heterogeneity might be related to ability to form tumors, but not due to hierarchical organization. However, examinations of human acute myeloid leukemia (AML) have demonstrated that L-ICs are

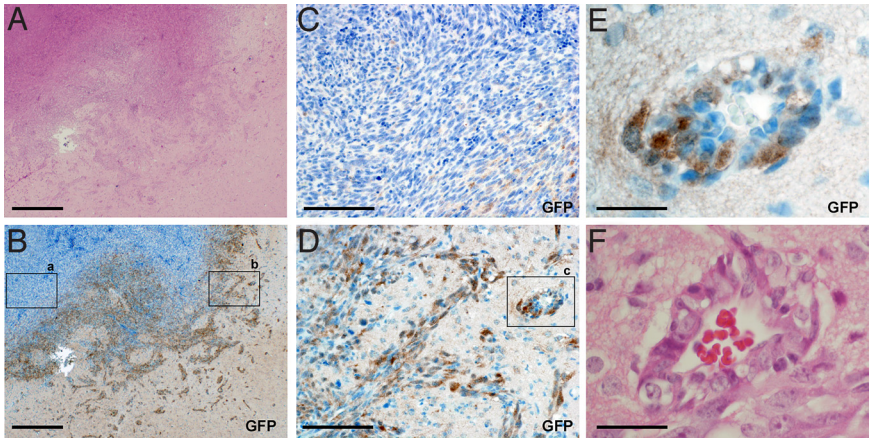

Fig. 4. Localization of T-ICs. Serial sections of a single-cell-derived tumor were stained with H&E (*A* and *F*) or anti-GFP (*B–E*) to identify T-ICs. (*A*) H&E staining of a tumor invading normal brain tissue. (*B*) Anti-GFP staining of the tissue in *A*. (*a* and *b*) Low-power views of areas shown at high power in *C* and *D*, respectively. (*E*) High-power view of area *c* in *D*. (*F*) H&E staining of *E*. (Scale bars: *A* and *B*, 1 mm; *C* and *D*, 200 μm; *E* and *F*, 50 μm.)

rare even when analyzed in NOD/SCID/Il2r$\gamma^{-/-}$ mice (27). A recent study of syngenic transplantation using mouse mammary tumor models also identified relatively rare T-ICs (28), suggesting that the frequencies of T-ICs may depend on type of cancer. Indeed, in our study, the frequency of GFP^{high} T-ICs varied greatly among individual brain tumors. In the case of a malignancy with a very high frequency of T-ICs (e.g., Fig. 3*A*, case 3), we surmise that most of the brain tumor cells present were "CSCs," as occurs in human melanomas. In other cases (e.g., Fig. 3*A*, case 1), the percentage of T-ICs was relatively low. Although we cannot yet be sure precisely what factors determine the frequency of T-ICs in a given tumor, we suspect that the stage of cancer progression (e.g., early versus late stage) is also important. Furthermore, we assume that the cell cycle status of T-ICs may also vary depending on the nature of the tumor. It has been previously reported that human leukemias include rare L-ICs, which showed slow cycling (27). In contrast, the GFP^{high} T-ICs in brain tumors analyzed in this study were actively cycling (Fig. S7). We hypothesize that, in the case of tumors showing a high frequency of T-ICs like our brain tumor model or human melanoma, T-ICs are actively cycling, resulting in very aggressive tumors.

Our NS-GFP-Tg system has allowed us to identify normal stem/progenitor cell populations in several different mouse tissues, including those responsible for neurogenesis and spermatogenesis (8). Although the population of cells strongly expressing GFP in each NS-GFP-Tg tissue may include progenitors, not only stem cells, we have observed a consistent relationship between GFP fluorescence intensity and degree of cellular maturation that has held across tissues. In addition, we also found that brain T-ICs were enriched by the NS-GFP system. Thus, both normal and tumor cells may use the same "stemness" programs. To investigate whether the NS-GFP system identify the "stemness" programs in tumor cell lines, we transfected the C6 glioma cell line with the NS-GFP construct and established stable clones. Although we found that most NS-GFP C6 cells in a single clone expressed GFP, as was the case in NS-GFP E14.5 embryonic brain, we did not observe differences in colony forming ability among subpopulations in C6 cells (Fig. S8). The inability to distinguish C6 T-ICs based on the NS-GFP expression is possibly due to that the fact that cultured C6 cells are more homogeneous than tumor tissue in vivo.

A key characteristic of human gliomas is their ability to invade normal brain tissue. As shown in Fig. 4, some tumor cells adjacent to blood vessels may lose GFP, suggesting that NS-GFP^{high} T-ICs may not be the only cells responsible for tumor invasion. However, we do not believe that NS-GFP^{low} cells adjacent to blood vessels contribute to tumor progression or expansion, because they lose the capacity for tumor-initiation, as shown in Fig. 3*D*. Glioma invasiveness is of clinical relevance, because brain tumor recurrence occurs most often within the surgical resection margin (12). Therefore, we believe that NS-GFP^{high} cells are primarily responsible for in invasion. The use of our stem cell concept-based system to further investigate tumor organization may increase our understanding of the nature of cancer and lead to the development of novel cancer therapies.

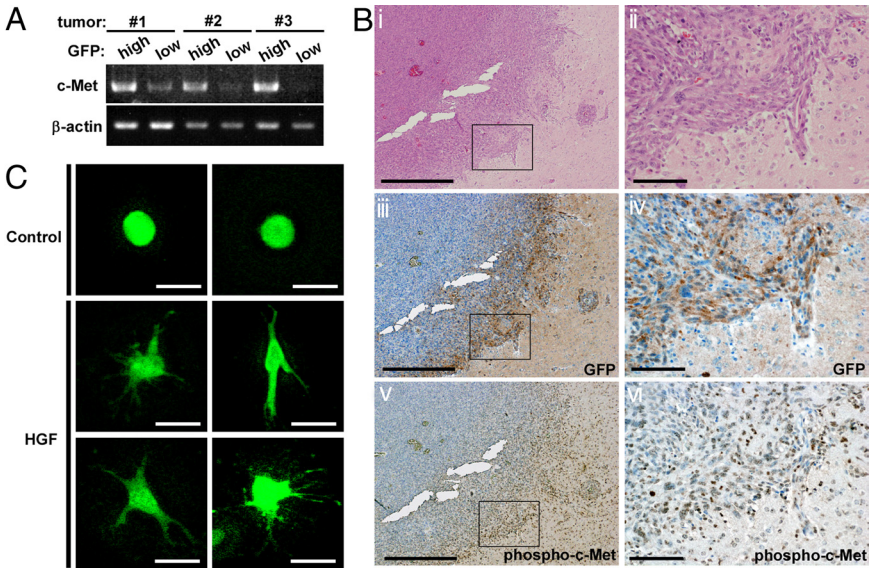

Fig. 5. Migration potential of T-ICs. (*A*) High expression of c-Met in GFP^{high} cells. Total RNA was purified from GFP^{high} and GFP^{low} cells isolated from three independent original tumors and c-Met mRNA levels were evaluated by RT-PCR. β-actin, control. (*B*) c-Met is phosphorylated in T-ICs. Serial sections of one of the single cell-derived tumors were subjected to H&E (*i* and *ii*); anti-GFP (*iii* and *iv*); and anti-phospho-c-Met (*v* and *vi*) staining. Magnified views of the areas indicated by the squares in *i*, *iii* and *v* are shown in *ii*, *iv*, and *vi*, respectively. (Scale bars: *i*, *iii*, *v*, 1 mm; *ii*, *iv*, *vi*, 200 μm.) (*C*) Migration of T-ICs in a collagen gel. Dissociated cells from a tumor were inoculated into either a plain collagen gel (control) or a collagen gel containing HGF (10 ng/mL) and incubated for 4 days. Representative GFP^{+} tumor cells with and without HGF in a collagen gel are shown. (Scale bars: 50 μm.)

Methods

Mice. All data presented in this study were obtained from experiments using heterozygous NS-GFP-Tg mice as described in ref. 8. $p16^{Ink4a+/-}/p19^{Arf+/-}$ mice were obtained from the Mouse Models of Human Cancers Consortium (MMHCC), National Cancer Institute-Frederick (29). All mice are of the C57BL/6 background. All animal procedures were performed in accordance with the animal care guidelines of Kanazawa University.

Generation of the Brain Tumor Model. A mutant K-ras^{G12V} gene was cloned into the retroviral vector pGCDN sap IRES huKO (30). Using Plat-E with *Lipofectin* Reagent (Invitrogen) (31), this vector was transfected into cells from the subventricular zone of NS-GFP-Tg/$p16^{Ink4a-/-}/p19^{Arf-/-}$ neonates (P4–5) that had been maintained under neurosphere culture conditions for 7days. The infected neurosphere cells were transplanted into the basal ganglia of 8–10-week-old C57BL/6 mice to generate brain tumors containing NS-GFP-Tg tumor cells.

Sphere Formation. Brain tumor cells or normal cells isolated from the brains of NS-GFP-Tg embryos or neonates and fractionated according to GFP fluorescence intensity. Cells from each fraction (1×10^3 cells per 100 μL) were cultured as described in ref. 32 in DMEM/F12-based serum-free growth medium containing insulin (25 μg/mL), transferrin (100 μg/mL), progesterone (20 nM), sodium selenate (30 nM), EGF (20 ng/mL), and bFGF (20 ng/mL). All reagents were from Sigma except for EGF, which was obtained from Stem Cell Technologies. On day 7 or 14, the number of spheres of diameter >50 μm was counted under a phase-contrast microscope.

Immunohistochemistry. Tumor or normal embryonic brain tissues were fixed in 4% paraformaldehyde and sections were immunostained with the following primary antibodies: mouse anti-nestin (BD), mouse anti-type III β-tubulin (TuJ1, Sigma), goat-anti-nucleostemin (R&D Systems), rabbit-anit-nucleostemin (Novus), rabbit-anti-GFP (Invitrogen), rabbit-anti-GFAP (Dakocytomation), and rabbit-anti-phosphorylated c-Met (Invitrogen). The staining signals for paraffin-embedded sections were visualized with peroxidase-conjugated secondary antibody (Amersham Biosciences), and counterstained with hematoxylin using the DAB Peroxidase Substrate Kit (VECTOR). The staining signals for frozen sections were visualized with the Alexa Fluor dye-conjugated secondary antibody: anti-mouse IgG, anti-rabbit IgG, or anti-goat IgG (Molecular Probes). Completed immunostaining was visualized using confocal microscopy (Olympus FV1000). For immunocytochemistry, cells were collected by flow cytometry and cytospin smears were prepared. Immunostaining was visualized using confocal microscopy. For visualization of nuclei, specimens were stained with DAPI or TOTO-3 (Molecular Probes).

Flow Cytometry. Tumor tissues were dissociated with 1 mg/mL collagenase (Sigma), whereas normal brain tissues were dissociated using a pipetting procedure. Cell sorting and flow cytometric analyses were performed using JSAN (Bay Bioscience). Sorted cells were resuspended in DMEM containing 10% FBS, washed once with medium, and prepared for further analysis. For transplantation or sphere formation experiments, we sorted subpopulations twice by flow cytometry. For some experiments, cytospin smears of the sorted cells were fixed with 4% paraformaldehyde.

Collagen Gel Invasiveness Assay. Freshly isolated tumor cells were suspended at 1×10^3 cells in 40 μL of ice-cold neutralized collagen type I from rat tail (2.4 mg/mL; BD) and incubated at 37 °C for 30 min. The resulting cell aggregates were further embedded in 500 μL of collagen type I solution (2.4 mg/mL) and solidified. The gels were floated on 500 μL of sphere formation medium containing EGF (20 ng/mL) and bFGF (20 ng/mL), with or without human recombinant HGF (10 ng/mL). This HGF was purifed from the conditioned medium of Chinese hamster ovary cells transfected with human HGF cDNA (22). The purity of the HGF was $>98\%$ as determined by SDS/PAGE and protein staining.

RT-PCR Analysis. RNA samples were purified from fractionated tumor cells (1×10^5) using the RNeasy kit (QIAGEN) and reverse-transcribed using the Advantage RT-for-PCR kit (Clontech). PCR was performed using a GeneAmp PCR system 9,700 (PE Applied Biosystems). The following primers were used: 5′-AGCATTTCTC-CGAGGTACGG-3′ and 5′-CATTGAGATCATTACTGGCT-3′ for c-Met; 5′-GTACCT-CAGATCCAGCCAGCAA-3′ and 5′-ATTCTTCCAGCTTGGGCAGC-3′ for prominin 1; 5′-AGGTCATCACTATTGGCAACGA-3′ and 5′-CACTTCATGATGGAATTGAATG-TAGTT-3′ for β-actin.

Statistical Analyses. *P* values were calculated using the unpaired Student's *t* test.

ACKNOWLEDGMENTS. We thank Dr. John E. Dick for helpful suggestions and critical reading of the manuscript, Miyako Takegami and Akiko Imamura for technical assistance, Dr. Toshio Kitamura for providing Plat-E, and Dr. Yoshinori Suzuki for help on the collagen gel invasiveness assay. This work was supported by Ministry of Education, Culture, Sports, Science and Technology, Japan Grant-in-Aid for Scientific Research on Priority Areas and Creative Scientific Research and for Cancer Research 17GS0419 (to A.H.) and a grant from the Ministry of Health, Labour and Welfare, Japan, for the Third-Term Comprehensive 10-year Strategy for Cancer Control (to A.H.) and in part by Kyowa Hakko Kirin Co. Ltd.

1. Pardal R, Clarke MF, Morrison SJ (2003) Applying the principles of stem-cell biology to cancer. *Nat Rev Cancer* 3:895–902.
2. Dick JE (2009) Looking ahead in cancer stem cell research. *Nat Biotechnol* 27:44–46.
3. Barabe F, Kennedy JA, Hope KJ, Dick JE (2007) Modeling the initiation and progression of human acute leukemia in mice. *Science* 316:600–604.
4. Al-Hajj M, Wicha MS, Benito-Hernandez A, Morrison SJ, Clarke MF (2003) Prospective identification of tumorigenic breast cancer cells. *Proc Natl Acad Sci USA* 100:3983–3988.
5. Singh SK, et al. (2004) Identification of human brain tumour initiating cells. *Nature* 432:396–401.
6. Schatton T, et al. (2008) Identification of cells initiating human melanomas. *Nature* 451:345–349.
7. Quintana E, et al. (2008) Efficient tumour formation by single human melanoma cells. *Nature* 456:593–598.
8. Ohmura M, et al. (2008) Identification of stem cells during prepubertal spermatogenesis via monitoring of nucleostemin promoter activity. *Stem Cells* 26:3237–3246.
9. Tsai RY, McKay RD (2002) A nucleolar mechanism controlling cell proliferation in stem cells and cancer cells. *Genes Dev* 16:2991–3003.
10. Beekman C, et al. (2006) Evolutionarily conserved role of nucleostemin: Controlling proliferation of stem/progenitor cells during early vertebrate development. *Mol Cell Biol* 26:9291–9301.
11. Maki N, et al. (2007) Rapid accumulation of nucleostemin in nucleolus during newt regeneration. *Dev Dyn* 236:941–950.
12. Nakada M, et al. (2007) Molecular targets of glioma invasion. *Cell Mol Life Sci* 64:458–478.
13. Holland EC, et al. (2000) Combined activation of Ras and Akt in neural progenitors induces glioblastoma formation in mice. *Nat Genet* 25:55–57.
14. Uhrbom L, et al. (2002) Ink4a-Arf loss cooperates with KRas activation in astrocytes and neural progenitors to generate glioblastomas of various morphologies depending on activated Akt. *Cancer Res* 62:5551–5558.
15. Bachoo RM, et al. (2002) Epidermal growth factor receptor and Ink4a/Arf: Convergent mechanisms governing terminal differentiation and transformation along the neural stem cell to astrocyte axis. *Cancer Cell* 1:269–277.
16. Marumoto T, et al. (2009) Development of a novel mouse glioma model using lentiviral vectors. *Nat Med* 15:110–116.
17. Louis DN, et al. (2007) The 2007 WHO classification of tumours of the central nervous system. *Acta Neuropathol* 114:97–109.
18. Merkle FT, Alvarez-Buylla A (2006) Neural stem cells in mammalian development. *Curr Opin Cell Biol* 18:704–709.
19. Lendahl U, Zimmerman LB, McKay RD (1990) CNS stem cells express a new class of intermediate filament protein. *Cell* 60:585–595.
20. Sakakibara S, et al. (1996) Mouse-Musashi-1, a neural RNA-binding protein highly enriched in the mammalian CNS stem cell. *Dev Biol* 176:230–242.
21. Kawaguchi A, et al. (2001) Nestin-EGFP transgenic mice: Visualization of the self-renewal and multipotency of CNS stem cells. *Mol Cell Neurosci* 17:259–273.
22. Nakamura T, et al. (1989) Molecular cloning and expression of human hepatocyte growth factor. *Nature* 342:440–443.
23. Matsumoto K, Nakamura T (2006) Hepatocyte growth factor and the Met system as a mediator of tumor-stromal interactions. *Int J Cancer* 119:477–483.
24. Brockmann MA, et al. (2003) Inhibition of intracerebral glioblastoma growth by local treatment with the scatter factor/hepatocyte growth factor-antagonist NK4. *Clin Cancer Res* 9:4578–4585.
25. Martens T, et al. (2006) A novel one-armed anti-c-Met antibody inhibits glioblastoma growth in vivo. *Clin Cancer Res* 12:6144–6152.
26. Tseng JR, et al. (2008) Preclinical efficacy of the c-Met inhibitor CE-355621 in a U87 MG mouse xenograft model evaluated by 18F-FDG small-animal PET. *J Nucl Med* 49:129–134.
27. Ishikawa F, et al. (2007) Chemotherapy-resistant human AML stem cells home to and engraft within the bone-marrow endosteal region. *Nat Biotechnol* 25:1315–1321.
28. Vaillant F, et al. (2008) The mammary progenitor marker CD61/beta3 integrin identifies cancer stem cells in mouse models of mammary tumorigenesis. *Cancer Res* 68:7711–7717.
29. Serrano M, et al. (1996) Role of the INK4a locus in tumor suppression and cell mortality. *Cell* 85:27–37.
30. Sanuki S, et al. (2008) A new red fluorescent protein that allows efficient marking of murine hematopoietic stem cells. *J Gene Med* 10:965–971.
31. Morita S, Kojima T, Kitamura T (2000) Plat-E: An efficient and stable system for transient packaging of retroviruses. *Gene Ther* 7:1063–1066.
32. Reynolds BA, Weiss S (1996) Clonal and population analyses demonstrate that an EGF-responsive mammalian embryonic CNS precursor is a stem cell. *Dev Biol* 175:1–13.